Reversible tuning of the surface state in a pseudobinary $Bi_2(Te\text{-}Se)_3$ topological insulator

Rui Jiang,[1,2] Lin-Lin Wang,[1] Mianliang Huang,[3] R. S. Dhaka,[1] Duane D. Johnson,[1,4]
Thomas A. Lograsso,[1] and Adam Kaminski[1,2,*]

[1]*Division of Materials Science and Engineering, Ames Laboratory, Ames, Iowa 50011, USA*
[2]*Department of Physics and Astronomy, Iowa State University, Ames, Iowa 50011, USA*
[3]*Materials and Metallurgical Engineering Department, South Dakota School of Mines, Rapid City, South Dakota 57701, USA*
[4]*Department of Materials Science and Engineering, Iowa State University, Ames, Iowa 50011, USA*

(Received 30 April 2012; published 10 August 2012)

We use angle-resolved photoemission spectroscopy to study a nontrivial surface state in a pseudobinary $Bi_2Te_{2.8}Se_{0.2}$ topological insulator. We show that, unlike previously studied binaries, this is an intrinsic topological insulator with the conduction bulk band residing well above the chemical potential. Our data indicate that under a good vacuum condition there are no significant aging effects for more than two weeks after cleaving. We also demonstrate that the shift of the Kramers point at low temperature is caused by UV-assisted absorption of molecular hydrogen. Our findings pave the way for applications of these materials in devices and present an easy scheme to tune their properties.

DOI: 10.1103/PhysRevB.86.085112 PACS number(s): 73.22.Gk, 73.20.−r

I. INTRODUCTION

The prediction and subsequent discovery of a surface state with a nontrivial spin structure in topological insulators[1,2] hold great promise for revolutionizing spintronics and quantum computing. Such a surface state has very unique properties as each electronic state in the momentum space is occupied by a single electron, unlike in traditional metals, where two electrons with opposite spin reside at each momentum point. This leads to unusual spin structure at the chemical potential, where electrons at opposite momentum have also an opposite spin. This obviously causes strong suppression of backscattering.

While several studies employing scanning tunnel microscope (STM) and angle-resolved photoemission spectroscopy (ARPES) techniques indeed show that electrons are immune to backscattering and nonmagnetic impurities,[3,4] the magnetic impurities, which break time-reversal symmetry, can create additional surface states with an odd number of Dirac fermions[5] and form a gap at the Kramers point.[6] Other studies of the effects of magnetic and nonmagnetic impurities on scattering rate[7] revealed that there is little difference between those two kinds of impurities.

The nontrivial surface state can surprisingly survive exposure to atmospheric pressure.[8] However, the electronic properties of the topological insulator were shown to change significantly in vacuum with time[8–11] with a typical time scale of hours or even minutes after cleaving, usually resulting in the formation of two-dimensional (2D) electron gas. One study also demonstrated that in some cases the carrier concentration may vary with photon energy used.[12] The delicate nature of the nontrivial surface state presents therefore a series of challenges, such as long-term stability and tunability, before it can be utilized in a new class of devices. In addition to the most popular topological insulators, Bi_2Se_3 and Bi_2Te_3, the recently grown $Bi_2(Te\text{-}Se)_3$ materials show surprisingly large bulk resistivity[13] and low carrier concentration.[14] By doping Sb into this material, the Dirac cone can be tuned from an n-type to a p-type topological insulator.[15]

Here we demonstrate that under good vacuum conditions the electronic structure of the surface state in $Bi_2Te_{2.8}Se_{0.2}$ remains unchanged over a period of two weeks even after temperature cycling. Compositions of more Te-rich than Bi_2Te_2Se display large low-temperature resistivity (>1 Ωcm)[16] and thus the lowest contribution from the bulk band to the electronic structure. We also show that this material is a "true" topological insulator, with the bulk conduction band located well above the chemical potential, and its electronic properties can be reversibly tuned by UV-assisted absorption of atomic hydrogen. This presents a simple way to tune the carrier concentration at the surface by adjusting the device temperature in a low-pressure hydrogen atmosphere.

II. EXPERIMENTAL DETAILS

Single crystals were grown using the proper ratio of the high-purity metals bismuth (99.999 %), selenium (99.999%), and tellurium (99.999%), which were sealed in a quartz tube and melted into an ingot in an induction furnace to homogenize the composition. The ingot was then sealed in a quartz tube with a larger diameter and loaded into a Bridgman furnace. A crystal was grown by withdrawing the quartz tube at 1 mm/h after being heated to 800 °C. The chemistry of the sample was determined using electron probe microanalysis (EPMA).

ARPES data were acquired using a laboratory-based system consisting of a Scienta SES2002 electron analyzer and a GammaData helium UV lamp. Samples were cleaved *in situ* at room temperature with base pressure in the vacuum system at 5×10^{-11} Torr. All data were acquired using the HeI line with a photon energy of 21.2 eV. The angular resolution was 0.13° along and ∼0.5° perpendicular to the direction of the analyzer slits. The energy resolution was set at ∼6 meV. Custom-designed refocusing optics enabled us to accumulate high-statistics spectra in a short time to study sample aging effects. The results were reproduced on several samples and temperature cycles.

All DFT calculations were done using VASP[17] on the (1×1) surface unit cell for $Bi_2Te_3(0001)$ with a slab of five atomic layers and 12 Å of vacuum. The bottom two layers are fixed at bulk positions, and the top three layers are free to relax until

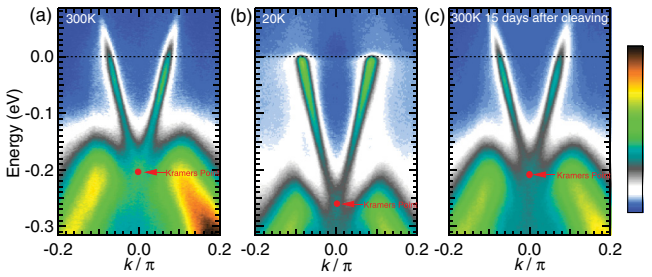

FIG. 1. (Color online) Long-term stability of the Dirac cone and temperature-induced changes in $Bi_2Te_{2.8}Se_{0.2}$. (a) Intensity plot along the high-symmetry direction at 300 K shortly after cleaving. (b) Data from the same cleave after cooling to 20 K. The band moves to higher binding energy caused by electron doping. (c) Data from the same cleave as in (a) and (b) at 300 K after 15 days of continuous measurement and temperature cycling, also showing that the carrier concentration and band position are the same as in the freshly cleaved sample.

the absolute magnitude of force on each atom is reduced below 0.02 eV/Å. A k-point mesh of $10 \times 10 \times 1$ with a Gaussian smearing of 0.05 eV and a kinetic energy cutoff of 300 eV was used.

III. RESULTS AND DISCUSSION

In Fig. 1, we examine the temperature dependence and stability of the surface band in the $Bi_2Te_{2.8}Se_{0.2}$ sample. Intensity plots show an almost linear dispersion of the surface band and an absence of the conduction bulk band at 300 and 20 K. The Kramers point, i.e., the apex of the Dirac cone, is below the Fermi surface, which indicates an n-type topological insulator. After cooling to 20 K [Fig. 1(b)] the band moves to higher binding energy. This behavior was previously attributed to phonon effects[18] or the photovoltaic effect.[19] Remarkably, after the sample was warmed up back to 300 K, the band structure recovered to its original state even though its surface was kept for 15 days in vacuum and exposed to UV and extensive temperature cycling [Fig. 1(c)].

We now focus on the cause of the changes in the band structure at low temperatures. In a fresh cleaved sample, the energy of Kramers point is −0.22 eV at 300 K [Fig. 1(a)]. We performed a large number of consecutive measurements for each of the sample temperatures, with results shown in Figure 2. In Figs. 2(a)–(d), we plot the ARPES intensity at various temperatures and exposure times. After the sample was kept at 20 K for 90 h we could observe the bulk conduction band, which, for a clean surface, demonstrates that the chemical potential is located within the bulk band gap. In Fig. 2(e), we show the evolution of the binding energy of the Kramers point with time and temperature. Each data point represents a separate measurement, and arrows mark the increase in sample temperature. When the sample was kept at 20 K, the Kramers point moved to higher binding energies, consistent with electron doping of the surface state. The process is relatively slow, which excludes scenarios involving phonons[18] or the photovoltaic effect.[19] The associated large time constant

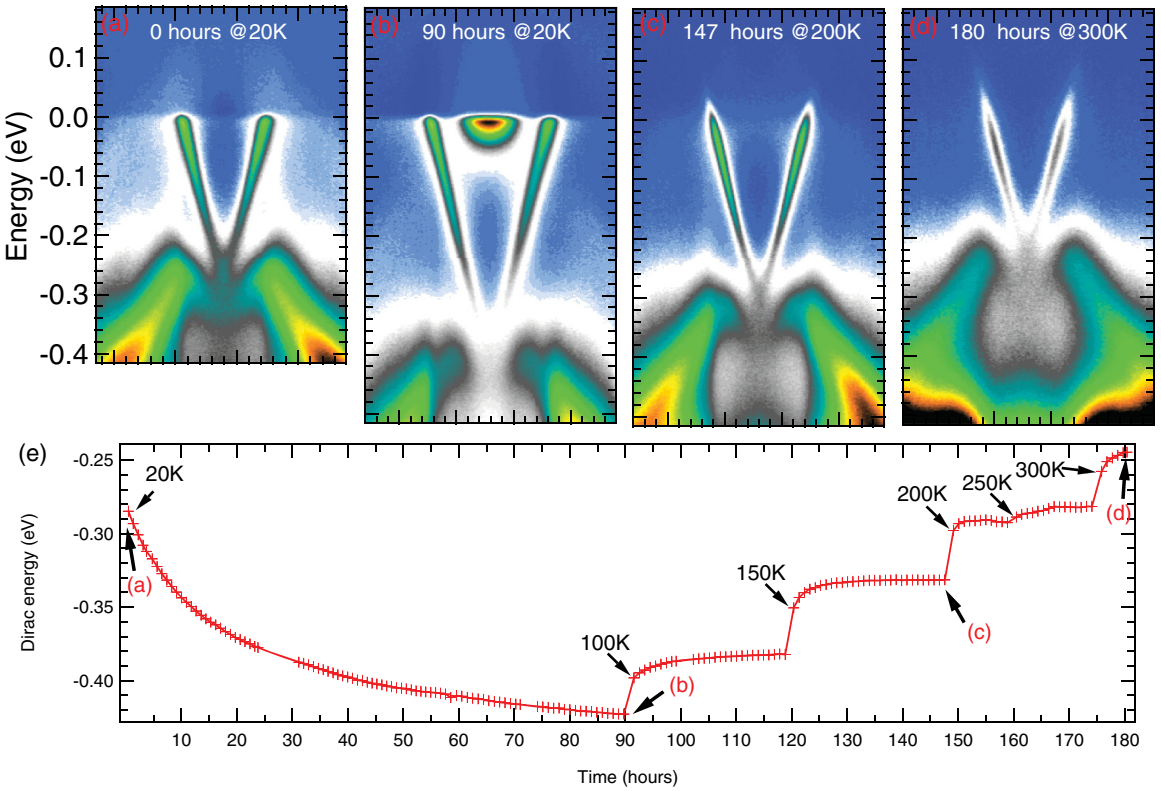

FIG. 2. (Color online) Evolution of the band structure with time and temperature. (a)–(d) Intensity plot at temperatures and times indicated by arrows in (e). (e) Binding energy of the Kramers point as a function of time upon temperature cycling. Arrows mark the first measurement at a given temperature.

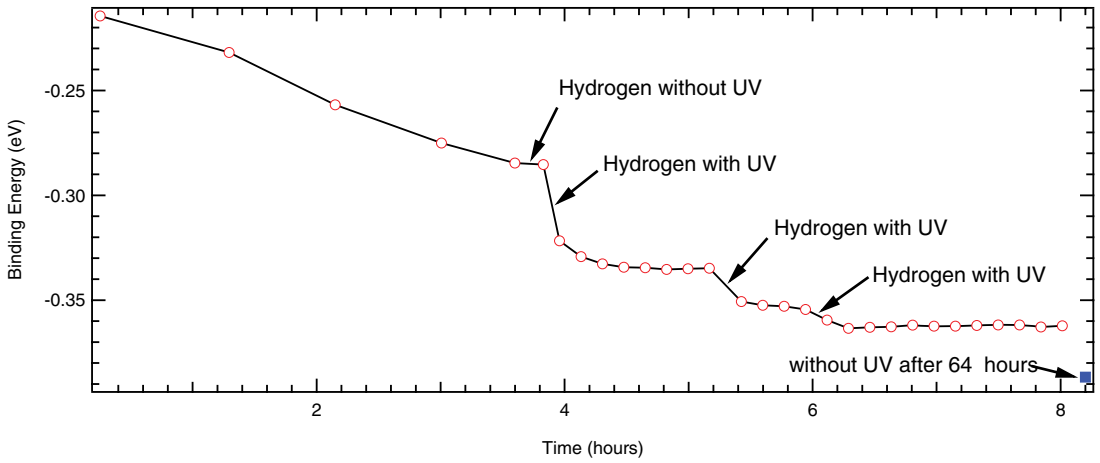

FIG. 3. (Color online) The effects of hydrogen and UV exposure. All measurements were preformed with the sample at 20 K. The black arrows indicate a brief increase of hydrogen pressure (1×10^{-7} Torr for 10 s). The blue square indicates the binding energy of the Kramers point after 64 h without UV light.

suggests chemical doping of the surface as the origin. We note that the changes significantly slow down with time, indicating saturation effects which are most likely caused by the reduction of the sticking coefficient with increased coverage. The reverse effect, with a similar time constant, occurs upon warming up. Here, we rapidly increase the sample temperature to values indicated by the arrows and continuously perform multiple consecutive measurements at each temperature. The carrier concentration decreases with increasing temperature. In each case, a saturation level is reached when the sample is kept at a fixed temperature for a sufficiently long time.

The most likely suspect for the change of carrier concentration is the absorption of hydrogen. Even in the best vacuum system made of stainless steel, hydrogen is omnipresent. Upon cooling, it can condense onto the surface and donate electrons to the surface state. The binding energy of molecular hydrogen is quite low (∼50 meV). It is possible, however, that UV light used for ARPES is causing its dissociation at the surface to atomic hydrogen, which has a much larger binding energy. To validate our assertion about the origin of the shift, we introduced a small amount of hydrogen into our vacuum system with and without UV. The binding energy of the Kramers point during this process is shown in Fig. 3. At the beginning of measurement, without the additional hydrogen, the binding energy of the Kramers point increased as in the previous case and shifted downward by about 70 meV. We injected hydrogen with the UV light switched off for 10 s at 10^{-7} Torr at the time marked by the black arrow in Fig. 3. We did not observe any significant change after injection. Then we injected the same amount of hydrogen in the presence of UV light. Under those conditions the band shifted in energy by 36 meV, as measured immediately after injection. We repeated this process two more times. The drop is obvious each time, but with decreasing magnitude, indicating saturation of hydrogen on the surface of sample.

To support our proposition that the origin of the electron doping and downward shift of the Dirac point are due to absorption of atomic H, we used density functional theory (DFT)[20,21] to calculate the adsorption of H_2 and H on the $Bi_2Te_3(0001)$ surface. Figure 4 shows the DFT adsorption energy of H_2 as a function of distance to the surface with different exchange-correlation functionals at the hcp site with an out-of-plane orientation for H_2. The data clearly show that the interaction between H_2 and the $Bi_2Te_3(0001)$ surface is of the van der Waals type. Perdew-Wang exchange and correlation functional (PW91)[22] gives a very weak binding of −27 meV at 3.5 Å, and local-density approximation (LDA)[23] gives a stronger binding of −82 meV at 2.5 Å, which is closer to −72 meV at 3.2 Å from the more accurate description of the system by the van der Waals exchange-correlation functional.[24] Upon full relaxation, the bond length of the adsorbed H_2 is 0.77 Å, only slightly longer than the 0.75 Å of the free H_2 molecule. The relaxation of the surface atoms is negligible. The adsorption energy at the three adsorption sites [fcc, bridge (brg), and top] is 5, 11, and 36 meV higher than the hcp site, respectively. The difference in adsorption energy on the same site with different orientations of H_2 is less than 5 meV.

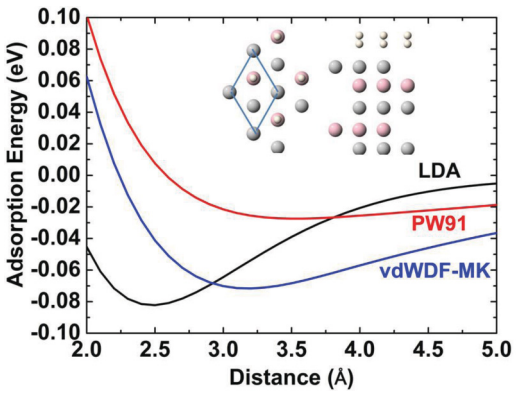

FIG. 4. (Color online) Adsorption energy of H_2 on $Bi_2Te_3(0001)$ as a function of distance to the surface with LDA, PW91, and vdWDF-MK exchange-correlation functionals. The inset shows the top and side views of the relaxed structure. The (1×1) surface unit cell is highlighted in the top view. Red, gray, and white spheres stand for Bi, Te, and H, respectively.

In contrast, the interaction between atomic H and the $Bi_2Te_3(0001)$ surface is much stronger, with a binding energy of −1.41 eV at the brg site (in reference to a free atomic H), followed by −1.08, −0.99, and −0.92 eV at the top, fcc, and hcp sites, respectively. The space among the surface atoms can accommodate atomic H very well, and the adsorbed H is in a coplanar position to surface Te atoms at all sites, except the top site, giving a binding distance of 1.73 Å. Although the adsorption energy in reference to a free H_2 molecule is 1.02 eV, which means that H_2 does not dissociate on the $Bi_2Te_3(0001)$ surface, the presence of UV light during ARPES measurement can produce atomic H, as confirmed experimentally. As supporting evidence, we also directly calculated the shift of the Dirac point in the surface band with different H_2 coverage. The downward shift due to the weak H_2-surface interaction is about 20 meV, which is too small compared to the shift of 100 meV observed in experiment.

IV. CONCLUSIONS

We have carefully detailed that the topological insulator behavior of $Bi_2Te_{2.8}Se_{0.2}$ remains unchanged and/or controllable over extended periods under good vacuum conditions, distinct from commonly observed Rashba effects, for example. We also showed that the Dirac cone electronic properties can be reversibly tuned by UV-assisted adsorption of atomic hydrogen, where DFT calculations confirm the assisted energetics and adsorption characteristics.

ACKNOWLEDGMENTS

Research was supported by the US Department of Energy, Office of Basic Energy Sciences, Division of Materials Sciences and Engineering. Ames Laboratory is operated for the US Department of Energy by the Iowa State University under Contract No. DE-AC02-07CH11358.

*kaminski@ameslab.gov

[1] B. A. Bernevig, T. L. Hughes, and S.-C. Zhang, Science **314**, 1757 (2006).
[2] D. Hsieh, D. Qian, L. Wray, Y. Xia, Y. S. Hor, R. J. Cava, and M. Z. Hasan, Nature (London) **452**, 970 (2008).
[3] P. Roushan, J. Seo, C. V. Parker, Y. S. Hor, D. Hsieh, D. Qian, A. Richardella, M. Z. Hasan, R. J. Cava, and A. Yazdani, Nature (London) **460**, 1106 (2009).
[4] X.-L. Qi and S.-C. Zhang, Rev. Mod. Phys. **83**, 1057 (2011).
[5] L. A. Wray, S.-Y. Xu, Y. Xia, D. Hsieh, A. V. Fedorov, Y. S. Hor, R. J. Cava, A. Bansil, H. Lin, and M. Z. Hasan, Nat. Phys. **7**, 32 (2010).
[6] Y. L. Chen *et al.*, Science **329**, 659 (2010).
[7] T. Valla, Z. H. Pan, D. Gardner, Y. S. Lee, and S. Chu, Phys. Rev. Lett. **108**, 117601 (2012).
[8] C. Chen *et al.*, Proc. Natl. Acad. Sci. USA **109**, 3694 (2012).
[9] D. Hsieh *et al.*, Phys. Rev. Lett. **103**, 146401 (2009).
[10] Z. H. Zhu *et al.*, Phys. Rev. Lett. **107**, 186405 (2011).
[11] P. D. C. King *et al.*, Phys. Rev. Lett. **107**, 096802 (2011).
[12] A. A. Kordyuk, T. K. Kim, V. B. Zabolotnyy, D. V. Evtushinsky, M. Bauch, C. Hess, B. Buchner, H. Berger, and S. V. Borisenko, Phys. Rev. B **83**, 081303(R) (2011).
[13] Z. Ren, A. A. Taskin, S. Sasaki, K. Segawa, and Y. Ando, Phys. Rev. B **82**, 241306(R) (2010).
[14] S. Jia, H. Ji, E. Climent-Pascual, M. K. Fuccillo, M. E. Charles, J. Xiong, N. P. Ong, and R. J. Cava, Phys. Rev. B **84**, 235206 (2011).
[15] T. Arakane, T. Sato, S. Souma, K. Kosaka, K. Nakayama, M. Komatsu, T. Takahashi1, Z. Ren, K. Segawa, and Y. Ando, Nat. Commun. **3**, 636 (2012).
[16] L.-L. Wang *et al.* (unpublished).
[17] G. Kresse and J. Furthmüller, Phys. Rev. B **54**, 11169 (1996).
[18] Z. H. Pan, A. V. Fedorov, D. Gardner, Y. S. Lee, S. Chu, and T. Valla, Phys. Rev. Lett. **108**, 187001 (2012).
[19] S. R. Park *et al.*, New J. Phys. **13**, 013008 (2011).
[20] P. Hohenberg and W. Kohn, Phys. Rev. **136**, B864 (1964).
[21] W. Kohn and L. J. Sham, Phys. Rev. **140**, A1133 (1965).
[22] J. P. Perdew and Y. Wang, Phys. Rev. B **45**, 13244 (1992).
[23] J. P. Perdew and A. Zunger, Phys. Rev. B **23**, 5048 (1981).
[24] J. Klimes, D. R. Bowler, and A. Michaelides, Phys. Rev. B **83**, 195131 (2011).